

Journal of Biomedical Optics

BiomedicalOptics.SPIEDigitalLibrary.org

Extraction of heart rate from functional near-infrared spectroscopy in infants

Katherine L. Perdue
Alissa Westerlund
Sarah A. McCormick
Charles A. Nelson, III

Extraction of heart rate from functional near-infrared spectroscopy in infants

Katherine L. Perdue,^{a,b,*} Alissa Westerlund,^a Sarah A. McCormick,^a and Charles A. Nelson III^{a,b}

^aDivision of Developmental Medicine, Boston Children's Hospital, Boston, Massachusetts 02215

^bDepartment of Pediatrics, Harvard Medical School, Boston, Massachusetts 02115

Abstract. Changes in heart rate are a useful physiological measure in infant studies. We present an algorithm for calculating the heart rate (HR) from oxyhemoglobin pulsation in functional near-infrared spectroscopy (fNIRS) signals. The algorithm is applied to data collected from 10 infants, and the HR derived from the fNIRS signals is compared against the HR as calculated by electrocardiography. We show high agreement between the two HR signals for all infants ($r > 0.90$), and also compare stimulus-related HR responses as measured by the two methods and find good agreement despite high levels of movement in the infants. This algorithm can be used to measure changes in HR in infants participating in fNIRS studies without the need for additional HR sensors.

© 2014 Society of Photo-Optical Instrumentation Engineers (SPIE) [DOI: [10.1117/1.JBO.19.6.067010](https://doi.org/10.1117/1.JBO.19.6.067010)]

Keywords: near-infrared spectroscopy; heart rate; infants.

Paper 140170R received Mar. 14, 2014; revised manuscript received May 19, 2014; accepted for publication Jun. 4, 2014; published online Jun. 27, 2014.

1 Introduction

The limited behavioral repertoire of young infants has made physiological recordings a useful measure of many aspects of infant development, particularly attention. One such measure that has proven particularly helpful is the recording of heart rate (HR) and heart rate variability (HRV).^{1,2} After the age of 2 months, decreases in HR, or decelerations, have been interpreted as an index of an orienting response; conversely, increases in HR (accelerations) are often interpreted as arousal. These changes in HR are on the timescale of several seconds and depend on the length of stimulus presentation. Over and above HR, HRV quantifies individual differences in autonomic responses to different stimuli and different stimulus classes. HRV can be quantified in short-term recordings over the course of several minutes or in long-term recordings which may last several hours.³

HR and HRV provide a measure of autonomic nervous system (ANS) activity, but do not directly reflect cortical activity. One of the many tools currently being employed as a means of direct visualization of the brain at work is functional near-infrared spectroscopy (fNIRS). fNIRS has been employed to measure cortical responses⁴ or resting-state connectivity^{5,6} in infants (also see recent reviews⁷⁻⁹). fNIRS has several advantages over other methods for functional brain imaging in infants. The method is relatively movement tolerant and allows infants to be seated comfortably in the presence of a caregiver. Additionally, infants' thin skulls allow light to easily reach the brain, and the resulting hemodynamic measurement can be compared to adult fNIRS responses or adult functional magnetic resonance imaging (fMRI).

In theory, simultaneous recordings of both fNIRS and HR would allow for complementary views of infants' autonomic and central nervous system responses to various task conditions. HR changes are a measure of attention and orienting; therefore,

having this information available would inform investigators of how the subjects perceive the task. HR is also thought to be modulated by subcortical structures that are not accessible with fNIRS; therefore, the addition of this measure adds complementary information to the fNIRS measurements. Conversely, fNIRS can provide more specific information about cortical regions involved in stimuli processing than can be inferred from changes in HR. Typically, HR is measured with electrocardiography (ECG), and is calculated by finding the time difference between subsequent R waves (R-R intervals) in the QRS complex. While there is no technical reason why simultaneous ECG and fNIRS cannot be performed, in practice this involves detailed setup procedures, including optodes placed on the head and electrodes placed on the chest. This setup is far from ideal when studying infants, who have very limited attention spans and ability to regulate their emotions. Thus, extracting the HR signal from the fNIRS signal would be preferable to separate ECG collection if it could be shown to have similar accuracy to using additional ECG sensors.

Prior work has shown that HR can be reliably extracted from the fNIRS signal in adults.¹⁰ However, extracting the HR from infant fNIRS presents additional challenges not present in the adult paradigm. Infants cannot be instructed to remain still during recording, resulting in high levels of movement artifacts in infant fNIRS data. Infants also have a faster resting HR than adults, which could potentially impact HR extraction algorithms. HRs of 180 beats per minute (BPM) or 3 Hz are not unusual in resting infants.² Signals on this timescale are considerably faster than the usual hemodynamic timescale that fNIRS instruments' sampling rates are optimized to capture. Additionally, infants have thinner skull and scalp tissue layers, which could be potentially problematic if most of the cardiac pulsation is coming from these layers, although cardiac pulsation has been inferred in the brain itself using fMRI.¹¹ Ideally, the program to extract the HR from the

*Address all correspondence to: Katherine Perdue, E-mail: Katherine.Perdue@childrens.harvard.edu

fNIRS signal would be freely available and able to be used on data collected with different instruments.

In this work, we propose an algorithm for extracting instantaneous HR from the fNIRS signal, and apply the method to fNIRS data collected from 10 infants. We validate the method with a simultaneous ECG, and apply the HR extraction method to calculate a stimulus-induced change in HR. We show that infant HR can be reliably and robustly extracted from fNIRS data collected for cognitive studies in infants, eliminating the need for ECG sensors and allowing for additional information to be extracted from fNIRS data that have already been collected for other purposes.

2 Methods

2.1 Functional Near-Infrared Spectroscopy and Electrocardiography Data Collection

A Hitachi ETG-4000 NIRS system was used to collect the fNIRS data. The probe design included 18 sources and 15 detectors arranged to cover the frontal, parietal, and temporal cortices with 3 cm source-detector distances. Continuous wave sources were at 695 and 830 nm. The probe layout and 46 resulting channels are shown in Fig. 1, along with a schematic of the positioning of the probe on the head and a photograph of the probe on a subject. Data were collected at 10 Hz.

ECG was recorded using a three-lead Biopac wireless Nomadix system (BIOPAC Systems, Inc., Goleta, CA) with a sampling frequency of 1000 Hz. Leads were attached using disposable sticker electrodes. Accelerometer data were also collected using a triaxial accelerometer (TSD109C1, BIOPAC Systems, Inc., Goleta, CA) attached to the forehead portion of the NIRS cap. The accelerometer was used to quantify infant head motion during the stimulus presentation. The accelerometer data were numerically integrated and combined across dimensions to provide a nondirectional measure of speed at each time point. It is worth noting that with our sensor on the fNIRS probe, the motion we are quantifying is the movement of the head only, and movements of the extremities will not be recorded unless it also causes head motion.

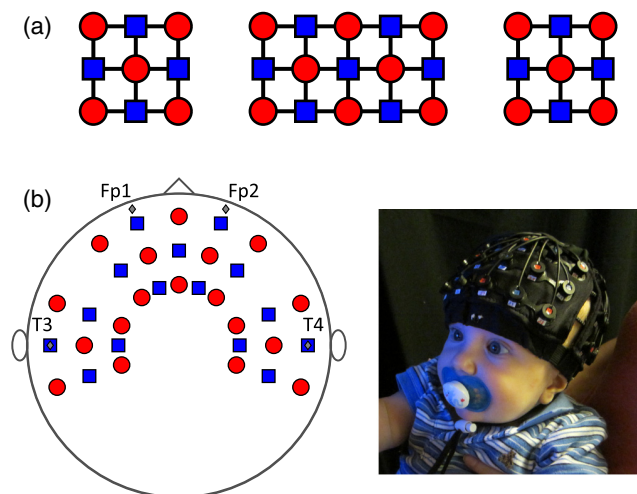


Fig. 1 Sources are red circles, detectors are blue squares. (a) Probe with source and detector locations showing 3 cm spacing between source detector pairs, (b) left: Schematic of probe on flattened head showing probe locations compared to anatomical landmarks and EEG landmarks (diamonds), (b) probe on subject.

2.2 Participants and Stimulus Design

Infants were recruited from a registry of local births to participate in a longitudinal study of emotion processing. The participants were typically developing and had no known prenatal or perinatal complications. The experimental protocol was approved by the IRB of Boston Children's Hospital, and informed consent was received from parents before beginning the sessions. The 10 participants in this study were 7-month-old-infants (7 males, $M_{\text{age}} = 208.8$ days, $SD = 4.2$). An additional two infants were tested but refused the fNIRS head probe. No infants refused the ECG sensors. The infants were held on their caregiver's lap while photographs of emotional faces ($N = 6$) or animals ($N = 4$) were presented on a computer screen at a distance of approximately 63 cm. The pictures were presented in a block design, with five photographs of duration 1 s presented per block and a randomly generated interstimulus interval of 200 to 400 ms between images. Stimulus blocks were followed by a 10 s animation of abstract shapes. A total of 30 stimulus blocks were presented to each infant as tolerated with breaks as necessary. The overall length of fNIRS recordings was between 7.5 and 14.5 min. Sessions were video recorded, and the videos were used to assess if the infants were looking at the stimulus while it was on the screen as a measure of attention. Videos were coded offline and a block was included in the stimulus-related averages if the infants viewed at least 3 of the 5 presented photographs.

2.3 Electrocardiography Heart Rate Extraction

ECG R-R intervals were determined using a modified Pan-Tompkins algorithm¹² implemented in AcqKnowledge software v4.2 (BIOPAC Systems, Inc., Goleta, CA). Manual correction was performed for dropped or spurious beats according to the instructions presented with the software. The HR data were then low-pass filtered with a cutoff frequency of 0.3 Hz to eliminate high frequency noise using a third-order IIR Butterworth filter applied in the forward and reverse directions to avoid phase distortion. The low-pass filter cutoff frequency was selected through systematic parameter variation. Sections of ECG data where the HR could not be calculated due to large artifacts were eliminated from further comparison with the fNIRS HR estimates. Bad sections were found in 5 of the 10 subjects, and in those subjects the mean length of the removed segments represented 4% of the total data length.

2.4 Functional Near-Infrared Spectroscopy Heart Rate Extraction Algorithm

The fNIRS raw data were converted to changes in chromophore concentration using the modified Beer-Lambert law as implemented in HOMER2¹³ after low-pass filtering with a third-order IIR Butterworth filter with a cutoff frequency of 4 Hz. The filter was applied in the forward and reverse directions to avoid phase distortion. The HR was extracted from each channel, and the channels with HR components were combined to create an overall estimate of the HR from the fNIRS recordings. The automated channel selection algorithm avoids experimenter bias in channel selection and allows the algorithm to be applied to datasets that do not have ECG for comparison and channel selection. The two main components of the fNIRS HR algorithm are, therefore, the channel selection component and the HR

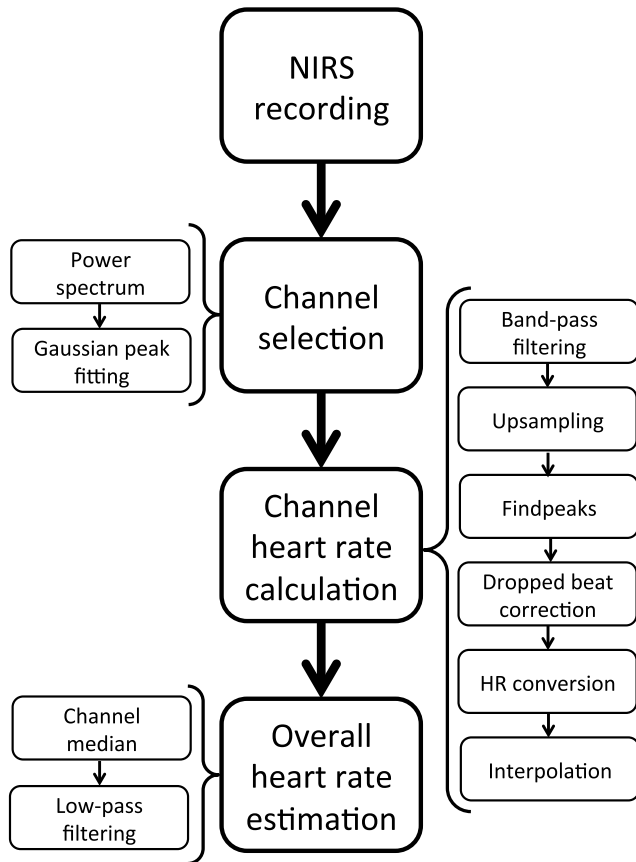


Fig. 2 Schematic showing the algorithm for estimating HR from fNIRS signal. The main steps in the algorithm are shown in the central path with details for each step on the sides.

extraction itself. A schematic of the algorithm for calculating the HR from the NIRS data is presented in Fig. 2. The algorithm parameters were systematically explored and values were chosen that optimized correspondence between the fNIRS and ECG HR signals.

2.4.1 Functional near-infrared spectroscopy channel selection

Channels with cardiac components were identified in the frequency domain. The multitaper method (MTM) power spectral density (PSD) estimate for each channel was calculated using the PSD MTM (PMTM) function in MATLAB® R2012b (The MathWorks Inc., Natick, Massachusetts). The multitaper method was used to estimate the PSD due to its excellent statistical properties including minimized bias and low variance.¹⁴ A Gaussian was fit to each spectrum using the FMINSEARCH function in MATLAB with the maximum in the power spectrum as the initial guess of the central frequency. Channels with Gaussian peaks of more than 6 dB in the infant HR range of 1.5–3.5 Hz were deemed as having sufficient cardiac signal to be included in future analysis. The peak height of 6 dB was chosen using a systematic parameter variation. Additionally, channels were marked bad if they had a signal of less than 2% of the raw intensity range or more than 98% of the raw intensity range for at least 5 s during the recording, indicating low-light intensity signal, or a railed signal.

2.4.2 Functional near-infrared spectroscopy heart rate calculation

The HR was initially estimated for each channel separately. First, the oxyhemoglobin (HbO) data for each selected channel were upsampled from 10 to 100 Hz using a polyphase implementation as provided with the RESAMPLE function in MATLAB. In adult fNIRS data, upsampling to 100 Hz from the relatively low-initial sampling frequency of 10 Hz has been shown to improve accuracy in HR estimation due to the better time resolution of the estimation of the interbeat intervals.¹⁰ The HbO signal is often used in studies where a high physiological signal content is desired.¹¹ The HbO signal was filtered from 1.5 to 4 Hz using a third-order IIR Butterworth filter to eliminate motion artifacts and low-frequency components. Peaks in the HbO signal were found using the FINDPEAKS routine in the MATLAB signal processing toolbox, with a minimum spacing equivalent to 200 BPM. Interpeak intervals were calculated, and intervals which were longer than the mean interval plus three standard deviations were assumed to include dropped beats and were, therefore, divided in half. The standard deviation threshold was chosen using a systematic parameter variation. Instantaneous HR was calculated from the inverse of the peak differences times and interpolated to 20 Hz using the INTERP1 MATLAB routine. Finally, an overall HR estimate was calculated by taking the median HR over the selected channels at each time point, and the resulting time series was low-pass filtered with a third-order IIR Butterworth filter with a cutoff frequency of 0.3 Hz. The filter was applied in the forward and reverse directions to avoid phase distortion. The low-pass cutoff frequency was chosen using systematic parameter space exploration and was also required to match the low-pass filter of the ECG HR estimate.

2.5 Functional Near-Infrared Spectroscopy Heart Rate Algorithm Evaluation

The accuracy of the HR timecourse calculated from the fNIRS signal was quantified by calculating the normalized cross covariance r for the fNIRS HR trace and the ECG HR trace. The covariance was scaled; therefore, the autocovariance was 1 for each signal at time lag 0. The time lag between the two traces was allowed to vary, and the highest r value is reported along with the corresponding lag.

2.6 Stimulus-Related Heart Rate Changes

The mean HR response to the stimulus presentation was calculated by averaging over all stimulus blocks in each subject. The HR response was calculated relative to the baseline of -4 to -2 s prestimuli. Blocks were only included in the average if the subject was looking at the screen for at least 3 of the 5 presented images, as determined by reviewing the video recordings of the sessions. For comparison, the HR response was also calculated from the ECG signal with the same stimulus inclusion criteria. If HR was not recoverable from the ECG, the trial was eliminated from both the ECG and fNIRS averages. The root-mean-square (RMS) error is reported along with the highest covariance r and the corresponding lag. An overall group average response for the HR calculated from the ECG and from the fNIRS recordings was also calculated.

3 Results

3.1 Functional Near-Infrared Spectroscopy Algorithm Parameter Setting

Parameters that were systematically varied to choose the optimal values were Gaussian peak height, low-pass filter cutoff frequency, and dropped beat identification threshold. Changing the selected parameters affected the performance of the HR extraction algorithm as shown in Fig. 3, which shows how the algorithm performance changes when one parameter is systematically varied and the others are held constant at their optimal values. The analysis was performed both with the full dataset and with every unique subset of five infants (252 total subsets) to probe the robustness of the parameter setting.

The Gaussian peak height parameter is used to select which channels are included in the overall HR calculation by quantifying how much signal is in the frequency band where the cardiac signal is expected. As shown in Fig. 3, the correlation between the fNIRS and ECG HR estimates is not very sensitive to changes in the Gaussian peak parameter, with median correlation values all within 0.005 of each other. However, the percentage of channels included in the overall HR calculation is dependent on the parameter and declines sharply for a Gaussian peak threshold larger than 6 dB. Accordingly, the Gaussian peak threshold was set to 6 dB in the algorithm.

The dropped beats' threshold is a metric which determines how long an interbeat interval can be before it is assumed to have contained a dropped beat. The unit is standard deviations of the overall beat time, i.e., beats must be longer than the mean

interbeat interval plus the number of standard deviations in order to be classified as containing a dropped beat. The standard deviations are calculated for each subject individually to account for variability in resting HR. Low values of this parameter may cause true long interbeat intervals to be "corrected" i.e., split, while high values of this parameter may not catch all true dropped beats. As shown in Fig. 3, low values of this parameter do cause marked decreases in the correlation between the fNIRS and ECG HR traces, along with more than 25% of the beats in a session being marked as dropped. Increasing this parameter caused sharp increases in fNIRS and ECG HR correlations and decreases in the percentage of beats marked as dropped. A threshold of three standard deviations was chosen to define dropped beats as it had the highest median correlation between ECG and fNIRS HR measures, which corresponded to approximately 1% of beats being classified as dropped.

The overall low-pass filter parameter shows how the agreement between fNIRS and ECG HR measures depends on the frequency content in the HR signal. For the purposes of looking at task-related changes in HR, we are looking for slow changes in the HR signal. We also expect that high frequency, non-physiological noise will persist in the HR signal as calculated with both methods, and we do not want to compare this noise between methods. Figure 3 does show a decrease in correlation between fNIRS HR and ECG HR as the low-pass filter cutoff frequency increases. However, we also expect that if filtering is too severe, the full extent of the HR response will not be included in the response estimate. In order to test how the low-pass filtering parameter impacts the mean over subjects, the

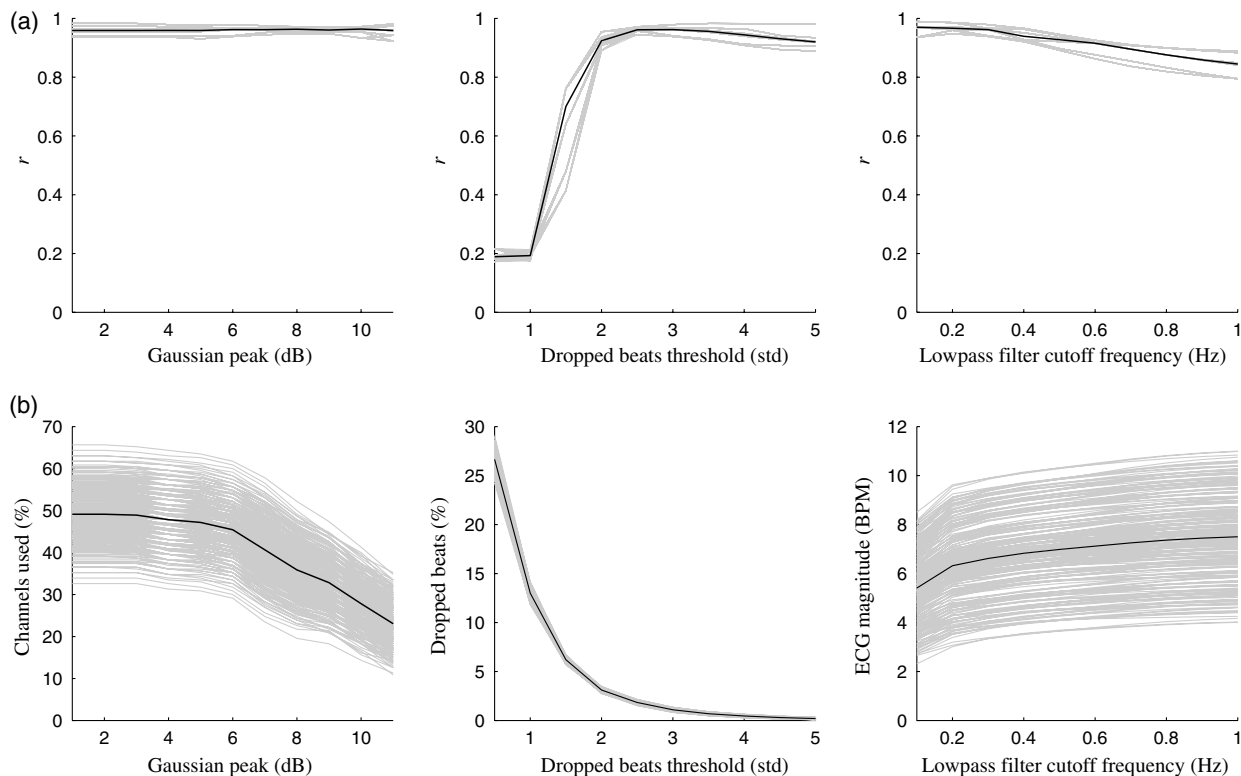


Fig. 3 Parameter setting results. (a) Row shows changes in median ECG HR and NIRS HR correlations with parameter variation, (b) row shows the mean percentage of channels used, mean percentage of dropped beats, and the mean magnitude of the ECG response. Black lines show the parameter curves from the full dataset, gray lines show the curves for every possible subset of five infants.

magnitude of the ECG response is used as a proxy for the overall response magnitude. The magnitude of this response increased with higher cutoff frequencies, perhaps due to the increased noise in the signal. However, it appears that choosing a low-pass cutoff frequency of 0.3 Hz retains high correlations between the NIRS and ECG HR signals without sacrificing too much signal magnitude; therefore, this value was chosen for use in further analyses.

3.2 Presence of Motion in Recordings

The infants' heads were moving during the recordings, with a group average speed of 0.099 m/s (group median of average speed is 0.077 m/s) over the sessions. A representative speed graph is shown in Fig. 4. This graph shows that there is frequent motion throughout the recording, and the speed is mostly less than 0.2 m/s. Speed was less than 0.2 m/s for 90% of the recording time on average, and greater than 0.05 m/s for 70% of the recording time on average. This speed distribution shows that the infant movements are frequent but usually not fast. Data were not excluded from further analysis on the basis of motion, but the accelerometer recordings were used to confirm that head motion was occurring and thus that the presented algorithm is robust to head motion.

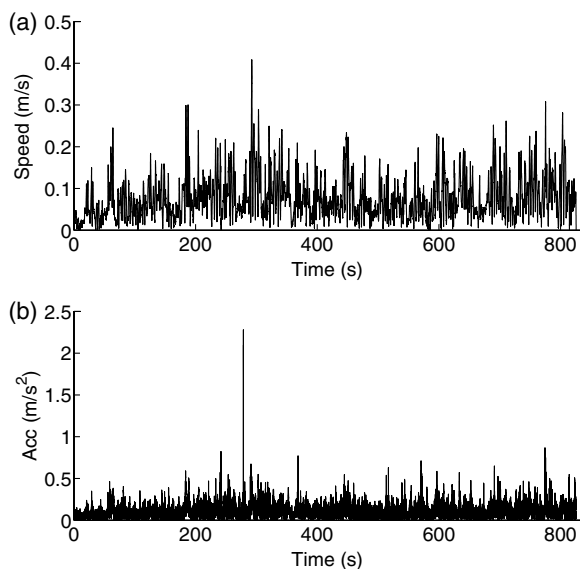


Fig. 4 Head speed (a) and acceleration (b) for infant 1 showing representative motion throughout the fNIRS session.

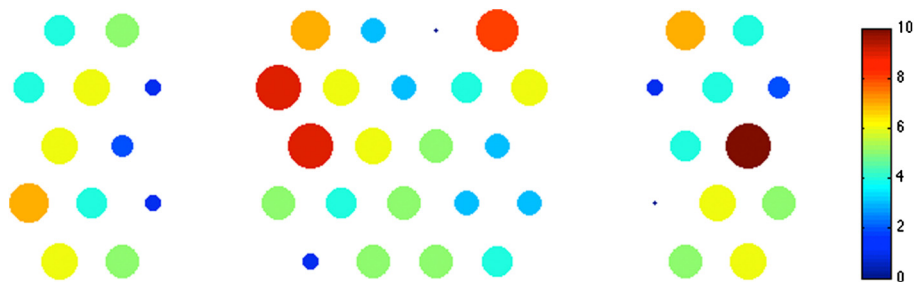


Fig. 5 Number of usable channels summed over 10 subjects, shown in their location on the optical head probe. Color and size of dot indicate the number of subjects that had a usable channel at each location.

3.3 Channel Selection

The number and locations of usable channels are shown in Fig. 5. The number of usable channels for each subject ranged from 9 to 38 out of 46 ($M = 20.9$ channels, $SD = 9.4$). The spatial distribution of usable channels in all subjects as shown in Fig. 4 indicates that there was not an overall spatial pattern where the usable channels were most likely to be located, indicating the benefit of picking channels based on individual signal characteristics over simply using a single channel in all subjects.

3.4 Overall Electrocardiography and Functional Near-Infrared Spectroscopy Heart Rate Correspondence

An example showing the correspondence between the ECG- and fNIRS-derived HR in a representative subject is shown in Fig. 6.

Correlations between ECG and fNIRS ranged from 0.9297 to 0.9872 with a median of 0.9618, and are presented for each subject in Table 1. For 9 of the 10 subjects, the fNIRS–ECG HR correlations derived from multiple HbO channels were higher than the best individual channel calculation, supporting the use of channel combination in the proposed algorithm. This result also implies that it is not necessary to guess the most accurate channel when ECG is not available for comparison, but that a group of useful channels can be selected with just the information from the fNIRS recording itself.

The HR fluctuations as recorded by fNIRS were delayed compared to those captured by the ECG. The overall delay for each subject ranged from 0.15 to 0.60 s, with a mean of 0.31 s. These lags for each participant are also listed in Table 1.

3.5 Stimulus-Related Heart Rate Responses

The group's mean change in HR during stimulus presentation is shown in Fig. 7. The magnitude of the decrease in HR with response to the stimulus is approximately 4 BPM. The HR deceleration begins prior to the stimulus onset, indicating the orientation of the infants to the screen before the stimulus is presented. Error metrics comparing the ECG HR and fNIRS HR for each infant are presented in Table 2. The correlations between the fNIRS and ECG HR remained high, with a minimum value of 0.9591, maximum of 0.9937, and median of 0.9811. The lags to the maximum correlation value ranged from 0 to 0.40 s, with a group mean of 0.21 s. The RMS error, calculated with the mean lag between fNIRS and ECG HR, had a median of 0.16 BPM and was below 1.3 BPM in all subjects, indicating good

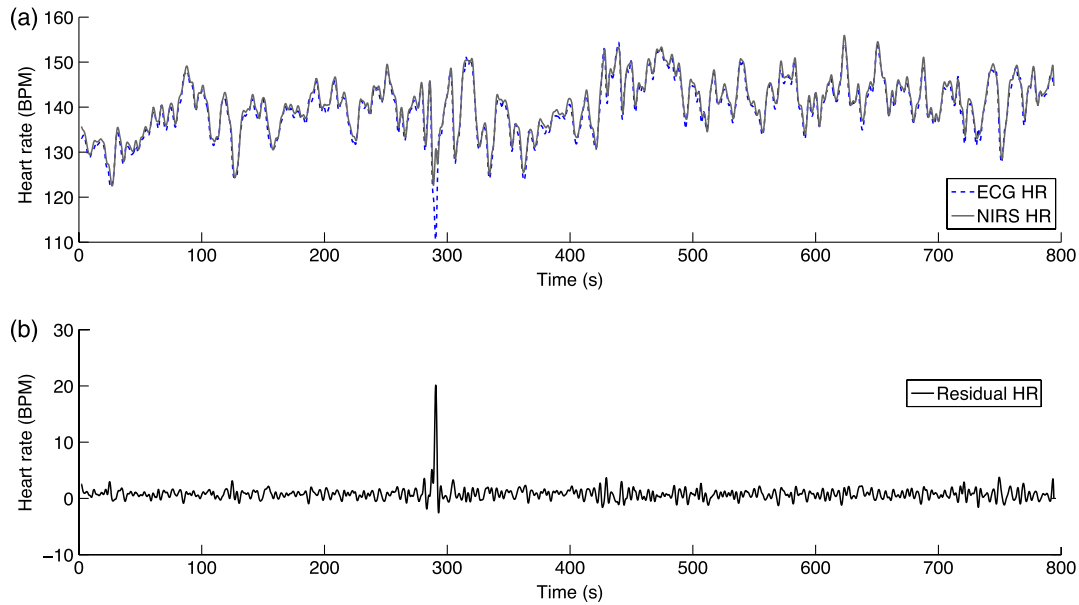


Fig. 6 ECG- and fNIRS-derived instantaneous heart rate over time in infant 1. (a) plot shows the HR as estimated by both ECG and NIRS, (b) plot shows the residual (NIRS-ECG).

agreement between the HR estimation for the two methods. The number of blocks used for each subject is also listed in Table 2.

4 Discussion

In this work, we describe an algorithm that accurately and robustly extracts the HR from the fNIRS signal. The ability to determine HR from the fNIRS signal eliminates the need for additional ECG sensors on infants, allowing for more information to be recorded with a simpler setup. HR information calculated from the fNIRS data allows for a greater understanding of infant responses to stimuli that is available from the standard fNIRS analysis, capturing both cortical and ANS responses.

Table 1 r values for optimal lag, maximum individual channel r , and optimal lag (fNIRS later than ECG).

Subject	r	Maximum individual channel r	Lag (s)
1	0.9787	0.9238	0.20
2	0.9872	0.9320	0.30
3	0.9307	0.8673	0.60
4	0.9297	0.9296	0.40
5	0.9382	0.9434	0.15
6	0.9624	0.9454	0.20
7	0.9855	0.9499	0.30
8	0.9408	0.8739	0.50
9	0.9612	0.9147	0.25
10	0.9658	0.9218	0.20

The correlations between ECG- and fNIRS-derived HR for the entire session and the stimulus-related responses were similar; however, the correlations for the stimulus-related responses were slightly higher, with a median of 0.9618 versus 0.9811. This higher correlation for the stimulus-related responses may reflect trials removed from the average due to infants looking away or otherwise not engaged in the stimulus. These removed trials may be more likely to include infant motion, and their removal may be the cause of the higher correspondence between the fNIRS and ECG stimulus-related signals.

A subject-dependent time lag of 0.15 to 0.60 s was found between the HR as recorded by the ECG and the fNIRS-derived HR. This delay is relatively short compared to the usual time-scale of hemodynamic measurements, which are often several seconds long. It is not surprising to see a delay in the HR as measured by fNIRS due to the time needed for the pressure wave from the contracting heart as measured by ECG to

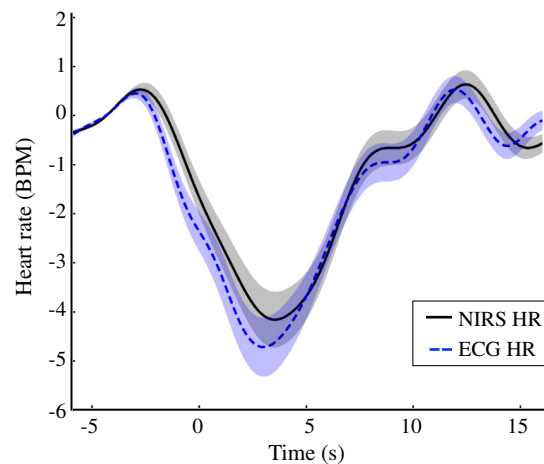


Fig. 7 Group mean stimulus-related change in heart rate as extracted from the fNIRS and ECG signals. Shaded areas show standard error of the mean.

Table 2 HR metrics for stimulus-related responses.

Subject	r	Lag (s)	RMS error (BPM)	Usable blocks
1	0.9937	0.15	0.14	23
2	0.9607	0.10	0.01	27
3	0.9754	0.40	0.39	18
4	0.9868	0	0.16	19
5	0.9754	0.40	0.19	28
6	0.9874	0.10	0.07	21
7	0.9889	0	0.11	23
8	0.9591	0.35	0.63	22
9	0.9691	0.40	1.28	22
10	0.9886	0.20	0.15	24

propagate to the head. This delay was subject dependent and may be influenced by factors such as subject size and stiffness of blood vessels. In our stimulus-induced HR responses, we also see a slight delay in the HR deceleration as measured by fNIRS as compared to the ECG, with a range from 0 to 0.40 s. However, the subject dependence of the optimal lag raises an issue if the method was applied on fNIRS data for which there was no ECG reference to calculate each subject's optimal lag between fNIRS HR and ECG HR. If we, instead, calculate correlations at only the fixed mean lag previously reported, the differences in the fNIRS–ECG correlations are small. For the total session metrics, the largest change in r is a decrease of 0.0074 if the mean lag instead of the maximum lag is used, and the median change is a decrease of 0.0013. For the stimulus-related responses, the largest change in r is a decrease of 0.0212 and the median change is a decrease of 0.0031. The small changes given a fixed delay between the fNIRS and ECG derived HR signals indicate that if ECG is not available for comparison, using a small fixed delay will still yield accurate fNIRS HR measures.

Movement-related noise affects the ECG and fNIRS signals differently. In our ECG signal, noise from infant motion is usually a sharp peak. The method for extracting HR from the ECG signal involves finding peaks on approximately the same time-scale as the movement artifacts. Because of the similarity of movement artifacts and the QRS complex as recorded by ECG, it might, in fact, be more accurate to calculate the HR based on photoplethysmography, usually via a pulse oximeter on the finger or foot, as compared to ECG. Motion artifacts in photoplethysmography signals are also sharp peaks, but the HR signal of interest is a slower wave corresponding to the pulsation in the blood vessels. The spectral separation of HR signals and motion artifacts in photoplethysmography have led some to postulate that it might be easier to get an artifact-free signal using photoplethysmography measures when recording in a high-motion environment, especially if accelerometer data to quantify motion is also available.¹⁵ However, this assumption is difficult to prove given that the HR as calculated from the ECG is used as the gold standard, and therefore is assumed to be defect free. In this study, we have looked at the

correspondence between the HR with ECG and fNIRS using the assumption that the ECG is correct. It is worth considering that in our high-noise environment, even with precautions to eliminate noise from the ECG signal manually, some noise may persist in the ECG signal, making disagreement between the fNIRS and ECG HR signals not solely due to defects in the fNIRS HR reconstruction. It is also possible that some of the difference between the two signals may reflect anatomical or physiological differences in the two recordings, i.e., the HR on the scalp may, in fact, be slightly different than the HR as measured by the heart contractions by ECG.

In our stimulus-related responses, we show that there is a decrease in HR with the presented stimulus, which has been shown elsewhere in infants as recorded by ECG.^{16,17} In this work, we have collapsed the stimulus-related HR responses over stimulus type to allow for easy comparison between ECG and fNIRS HR signals. However, differences in HR decelerations have been used to infer differences in attention to stimulus classes. The specific shape of the HR deceleration can be used to quantify the different attentional processes.¹⁸ The magnitude of the decrease in HR of about 4 BPM is similar to what has been reported elsewhere.¹⁷

The correlation between HR as recorded by ECG and the HR extracted from fNIRS is somewhat lower than has been reported elsewhere in adult data.¹⁰ However, the method presented here does not require signals to be free of movement artifact, which is a large advantage when infant applications are considered. Our algorithm also does not require the experimenter to select a particular channel of interest for the HR calculation, and instead uses all channels with a sufficient HR spectral content in the HbO signal. While the method presented here has been designed for infant data, there is no reason why it could not be applied to adult data as well with appropriate alteration of the expected HR frequency band. The algorithm might be especially useful in adult studies when a high degree of participant movement is expected during the session.

The availability of HR data from fNIRS allows for the possibility of simultaneous resting state fNIRS and respiratory sinus arrhythmia (RSA) studies using only fNIRS sensors due to the similar study designs of these protocols. Changes in RSA have been linked to clinical problems, such as sudden infant death syndrome,¹⁹ social developmental delays,² and autism.²⁰ RSA in infants have also been linked to other cognitive processes such as attention,²¹ emotion regulation,²² and behavioral measures such as temperament.²³ RSA has also been shown to be a particularly robust metric in infants due to the large changes in the HR as modulated by respiration. It has already been shown that RSA can be reliably calculated from the pulse oximetry signals.²⁴ While RSA was not quantified in this study due to the task-related experimental design, the method outlined in this paper suggests that it would be straightforward to combine resting-state fNIRS studies with a respiratory measure to do simultaneous cortical connectivity and RSA studies.

5 Conclusion

HR can be successfully recovered from fNIRS data in infant studies, eliminating the need for additional HR sensors. The algorithm presented here extracted the HR from the fNIRS signals with a correlation with the ECG HR of above 0.92 in all 10 infants. The algorithm was robust, as these results were achieved despite frequent infant head movements. The correlation between the HR estimated with both ECG and fNIRS was

high over the whole session and in the stimulus-related responses. The stimulus responses have an RMS error less than 1.3 BPM in all 10 infants. Extraction of HR from the fNIRS signals will also allow previously collected infant data to be reanalyzed for measures of attention, increasing the utility of fNIRS as a simultaneous measure of infant physiology and brain functioning.

Acknowledgments

The authors would like to thank the families for their participation. Assistance with data collection was provided by Lina Montoya and Ross Vanderwert. This work was financially supported by R01MH078829 and the Simons Foundation.

References

1. F. K. Graham and J. C. Jackson, "Arousal systems and infant heart rate responses," *Adv. Child Dev. Behav.* **5**, 59–117 (1970).
2. J. E. Richards and D. Cameron, "Infant heart-rate variability and behavioral developmental status," *Infant Behav. Dev.* **12**(1), 45–48 (1989).
3. M. Malik et al., "Heart rate variability standards of measurement, physiological interpretation, and clinical use," *Eur. Heart J.* **17**(3), 354–381 (1996).
4. T. Wilcox et al., "Using near-infrared spectroscopy to assess neural activation during object processing in infants," *J. Biomed. Opt.* **10**(1), 011010–0110109 (2005).
5. F. Homae et al., "Development of global cortical networks in early infancy," *J. Neurosci.: Off. J. Soc. Neurosci.* **30**(14), 4877–4882 (2010).
6. B. Keehn et al., "Functional connectivity in the first year of life in infants at-risk for autism: a preliminary near-infrared spectroscopy study," *Fron. Hum. Neurosci.* **7**, 444 (2013).
7. S. Lloyd-Fox, A. Blasi, and C. E. Elwell, "Illuminating the developing brain: the past, present and future of functional near infrared spectroscopy," *Neurosci. Biobehav. Rev.* **34**(3), 269–284 (2010).
8. R. E. Vanderwert and C. A. Nelson, "The use of near-infrared spectroscopy in the study of typical and atypical development," *NeuroImage* **85**, 264–271 (2014).
9. S. Nagamitsu et al., "Functional near-infrared spectroscopy studies in children," *BioPsychoSoc. Med.* **6**(1), 7 (2012).
10. I. Trajkovic, F. Scholkmann, and M. Wolf, "Estimating and validating the interbeat intervals of the heart using near-infrared spectroscopy on the human forehead," *J. Biomed. Opt.* **16**(8), 087002 (2011).
11. Y. Tong and B. D. Frederick, "Time lag dependent multimodal processing of concurrent fMRI and near-infrared spectroscopy (NIRS) data suggests a global circulatory origin for low-frequency oscillation signals in human brain," *NeuroImage* **53**(2), 553–564 (2010).
12. J. Pan and W. J. Tompkins, "A Real-time QRS detection algorithm," *IEEE Trans. Biomed. Eng. BME-32(3), 230–236 (1985).*
13. T. J. Huppert et al., "HomER: a review of time-series analysis methods for near-infrared spectroscopy of the brain," *Appl. Opt.* **48**(10), D280–D298 (2009).
14. B. Babadi and E. N. Brown, "A review of multitaper spectral analysis," *IEEE Trans. Biomed. Eng.* **61**(5), 1555–1564 (2014).
15. G. Lu et al., "A comparison of photoplethysmography and ECG recording to analyse heart rate variability in healthy subjects," *J. Med. Eng. Technol.* **33**(8), 634–641 (2009).
16. M. L. Courage, G. D. Reynolds, and J. E. Richards, "Infants' attention to patterned stimuli: developmental change from 3 to 12 months of age," *Child Dev.* **77**(3), 680–695 (2006).
17. M. J. Peltola et al., "The emergence and stability of the attentional bias to fearful faces in infancy," *Infancy* **18**(6), 905–926 (2013).
18. J. E. Richards and B. J. Casey, "Heart rate variability during attention phases in young infants," *Psychophysiology* **28**(1), 43–53 (1991).
19. G. Sugihara et al., "Nonlinear control of heart rate variability in human infants," *Proc. Natl. Acad. Sci. USA.* **93**(6), 2608–2613 (1996).
20. E. Bal et al., "Emotion recognition in children with autism spectrum disorders: relations to eye gaze and autonomic state," *J. Autism Dev. Disord.* **40**(3), 358–370 (2010).
21. J. E. Richards and B. J. Casey, "Development of sustained visual attention in the human infant," in *Attention and Information Processing in Infants and Adults*, B. A. Campbell, H. Hayne, and R. Richardson, Eds., pp. 30–60, Erlbaum, Hillsdale, NJ (1992).
22. G. A. Moore and S. D. Calkins, "Infants' vagal regulation in the still-face paradigm is related to dyadic coordination of mother-infant interaction," *Dev. Psychol.* **40**(6), 1068–1080 (2004).
23. K. B. Burgess et al., "Infant attachment and temperament as predictors of subsequent externalizing problems and cardiac physiology," *J. Child Psychol. Psychiat.* **44**(6), 819–831 (2003).
24. S. Lu et al., "Can photoplethysmography variability serve as an alternative approach to obtain heart rate variability information?," *J. Clin. Monit. Comput.* **22**(1), 23–29 (2008).

Katherine L. Perdue received a BS in physics from Harvey Mudd College in 2005 and a PhD in engineering sciences from the Thayer School of Engineering at Dartmouth in 2012. Between degrees she worked as a research assistant at the Martinos Center for Biomedical Imaging at Massachusetts General Hospital. Currently, she is a postdoctoral research fellow at Boston Children's Hospital with research focused on developing imaging methods for pediatric brain research.

Charles A. Nelson III is a professor of Pediatrics and Neuroscience and professor of Psychology in Psychiatry at Harvard Medical School and holds the Richard David Scott Chair in Pediatric Developmental Medicine Research at Boston Children's Hospital. The Nelson Laboratory conducts research on a variety of problems in developmental cognitive neuroscience, with a particular focus on the effects of early experience on brain development and the development of autism. He has published over 250 peer-reviewed papers.

Biographies of the other authors are not available.